Proceedings of the ASME 2023 Conference on Smart Materials, Adaptive Structures and Intelligent Systems
SMASIS2023
September 11-12, 2023, Austin. Texas

SMASIS2023-108891

The Dual Role Of "Coffee-Ring" Effect In Colloidal Microchannel Formation

Ryan Dumont
Department of Mechanical Engineering, Kennesaw State University, Marietta, GA

Spandana Thammisetty
Department of Mechanical Engineering, Kennesaw State University, Marietta, GA

Bo Li
(Corresponding Author, e-mail: bli10@kennesaw.edu)
Department of Mechanical Engineering, Kennesaw State University, Marietta, GA

ABSTRACT

In order to address the challenges presented by future electronics with complex functionality and architecture, new materials and fabrication methods must be developed. In contrast to traditional top-down approaches, bottom-up self-assembly has emerged as a robust means of organizing nanoscopic building blocks into highly ordered structures and materials. In particular, topographical micropatterns are typically fabricated using complicated lithographic methods that are expensive and time-consuming and not suitable for high throughput manufacturing. Colloidal cracks, also known as colloidal microchannels, have been identified as a simple and robust strategy for the fabrication of scalable microchannels. Despite extensive theoretical modeling to understand the mechanism of crack formation, the influence of the "coffee-ring" effect on crack formation remains largely unexplored. Herein, we explore how the "coffee-ring" effect determines the colloidal microchannel formation by leveraging the kinetic control of the non-equilibrium deposition process of PS latex nanoparticles. Surprisingly, by tuning the particle size, we found the "coffee-ring" effect plays a dual role in determining the colloidal microchannel formation. In addition, temperature-concentration phase diagrams of colloidal microchannel formation are also provided in this work. Overall, the study presented offers crucial insights into controlling the self-assembly of colloidal particles to form microchannels, which is essential for the low-cost and large-scale fabrication of topographical templates. This study has important applications in microfluidics, geometry confinement for functional materials deposition, and alignment.

Keywords: Self-assembly, Colloidal Microchannels, Coffee-ring effects, Advanced Manufacturing

1. INTRODUCTION

In order to address the challenges presented by future electronics with complex functionality and architecture, new materials and fabrication methods must be developed. In contrast to traditional top-down approaches, bottom-up self-assembly has emerged as a robust means of organizing nanoscopic building blocks [1-2] into highly ordered structures and materials[3-4] for use in catalysis, optics, electronics, photonics, and sensors.[5-7] In addition, self-assembly offers a low-cost alternative to traditional fabrication methods and has been used to create a variety of self-assembled structures composed of different nanomaterials.[8-11] In this regard, because topographical micropatterns are typically fabricated using complicated lithographic methods that are expensive and time-consuming and not suitable for high throughput manufacturing, self-assembly of functional colloidal particles could address the challenge by providing a low-cost, large-scale method for topographical template preparation.

In particular, colloidal cracks, also known as colloidal microchannels, have been identified as a simple and robust strategy for the fabrication of scalable microchannels. Cracks are typically considered problematic and challenging in industries such as paint and coatings, as they are strongly unfavorable and lead to non-uniform film thickness.[12-13] Despite extensive theoretical modeling to understand the mechanism of crack formation, [14-17] the influence of the "coffee-ring" effect on crack formation remains largely unexplored. As a result, there are

limited methods to experimentally manipulate cracks upon drying, which would provide new opportunities for tailorability of crack morphology and regularity.[18]

The "coffee-ring" effect is a phenomenon where a droplet composed of a volatile solvent and non-volatile solutes leaves a ring-like deposit along the contact line during evaporation. This effect has significant implications in applications such as surface coating, solution printing, and inkjet printing processes. The mechanism of this phenomenon was first proposed by Deegan in 1997,[19] which could be divided into four basic steps: 1. An evaporation rate gradient at the air-solvent interface close to the contact line generates a capillary flow towards the contact line.[20-22] 2. Radial flows effectively transport the solute to the contact line.[23-25] 3. Due to the attraction between the substrate and solute, the solute deposits and forms a continuous line along the contact line. [26-27] 4. As the droplet continuously evaporates, the force induced by surface tension overcomes the pinning force, leading to the depinning of the contact line from the ring of deposited solute and jumping inward.[28] This process results in a concentric ring-like deposition pattern. To date, several studies have been conducted to investigate the use of evaporation for the rapid and cost-effective formation of well-ordered structures over large areas by utilizing the “coffee-ring“ effect.[29-43]

Herein, we explore how the “coffee-ring“ effect determines the colloidal microchannel formation by leveraging the kinetic control of the non-equilibrium deposition process of PS latex nanoparticles. Surprisingly, by tuning the particle size, we found the “coffee-ring“ effect plays a dual role in determining the colloidal microchannel formation. On one hand, the “coffee-ring“ effect results in a outward flux that carries colloidal particle to the contact line to form a continuous wet colloidal film, which later engenders colloidal microchannel fomrations upon drying. On the other hand, the “coffee-ring“ effect leads to accumulation of colloidal particles at the edge of droplet, which causes strong pinning of the contact line, and, therefore, renders the suppress of colloidal microchannel formation. The dual role of the the “coffee-ring“ effect requires judicious selection of the solution condition in order to yield relatively uniform colloidal microchannel formation. In addition, temperature-concentration phase diagrams of colloidal microchannel formation are also provided in this work. Overall, the study presented offers crucial insights into controlling the self-assembly of colloidal particles to form microchannels, which is essential for the low-cost and large-scale fabrication of topographical templates. This study has important applications in microfluidics, geometry confinement for functional materials deposition, and alignment.

2. MATERIALS AND METHODS

First, a droplet (15 μL in this work) of PS latex nanoparticle (50 nm) aqueous solution was deposited on Si water to allow free evaporation. The Si wafers were cut into small 2 cm^2 pieces, which were then cleaned with a mixed solution of 18M sulfuric acid for 12 hr, vigorously rinsed with DI water and blow-dried with N_2. The PS latex nanoparticles solutions was purchased from Thermo Scientific (c = 2.5 wt % particle solids) without further purification. Notably, the concentraition 100% means 2.5 wt% of PS latex nanoparticle in solution without any dilution, and concentation 60% means 0.6*2.5 wt% = 1.5wt%. The heating stage was built based on a Peltier stage, with resolution of 0.1℃, allowing for precise control of the evaporation process. materials and methods that have been used in the work must be stated clearly. Subtitles should be used when necessary.

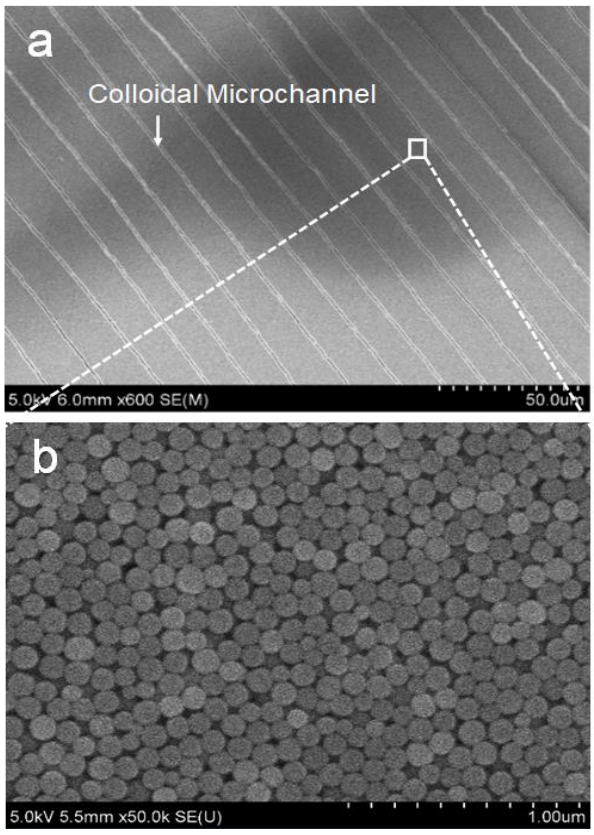

FIGURE 1: Scanning electron microscope (SEM) images of (a) colloidal microchannels formed by PS latex nanoparticles of 50 nm and (b) zoomed in image of the packing of PS latex nanoparticles

3. RESULTS AND DISCUSSION

During the evaporation of the droplet, the solvent molecules (i.e., water molecules) escape the droplet at different evaporation rates along the meniscus profile. The area close to the three-phase (i.e., water/substrate/air) contact line has the maximum evaporation rate, and the inner bulk has lower evaporation rate. As a result, an outward flux was generated inside of the droplet (so called “coffee-ring” effect), carrying PS latex nanoparticles moving towards the contact line. Due to the attractive interaction and the ultra-thin liquid film close to the contact line, PS latex nanoparticles were deposited at the edge. Simultaneously, if the contact moved inward during evaporation, a continuous wet colloidal film formed. Upon drying of the colloidal film, the internal stress generated by capillary stress lead to crack

formation (i.e., colloidal microchannels),[44] yielding regular colloidal microchannel pattern as shown in SEM image (Figure 1a), with colloidal microchannel pattern at much larger scale shown in optical microscope image (Figure 2a). Notably, the experimental conditions for Figure 2a and Figure 2b are 50℃/60% and 50℃/10% respectively, which detailed explanation provided in below. As shown in Figure 1b, even though the size PS latex nanoparticle is nearly uniform, they did not form closely packed structure (e.g., face centered cubic, FCC) within the colloidal film, suggesting that close packing of particles is not necessary for colloidal microchannel formation.

Importantly, the channel-to-channel distance λ_{c-c} is around 50 μm at the outer part of the colloidal film and decreases to around 10 μm at the inner part (Figure 2a). The λ_{c-c} could be determined by various factors, which was rationalized in our previous work:[45]

$$\lambda_{c-c} \sim 0.07 \left(\frac{20}{75} \left(\frac{3\gamma\eta_0}{E} \right)^{\frac{1}{2}} \frac{R(1-\phi)^2}{\mu\phi^2 H} \right)^{-0.8} \left(\frac{20R(1-\phi)^2}{75\mu\phi^2} \right) \left(\frac{3\gamma^3\eta_0}{E^3} \right)^{\frac{1}{4}}$$

where η_0 represents the dispersion viscosity of solvent in the colloidal thin film, H is the film thickness, γ is the surface tension, μ is the viscosity, E is the wet colloidal film evaporation rate, R is the radius and ϕ is the volume fraction of PS latex nanoparticle. Clearly, the key variable that was changed from the outer to inner part is the film thickness H. The freely evaporated droplet rendered more PS latex nanoparticle deposited close to the contact line due to the "coffee-ring" enhancement, which lead to higher film thickness. As a result, the channel-to-channel distance λ_{c-c} is much larger in the outer part.

However, the "coffee-ring" enhancement could yield a thick ring-like deposition around the edge while leaving few PS latex nanoparticle deposited inside the thick ring (Figure 2b). Consequently, no colloidal microchannel formed inside the ring. To this end, we summarized the temperautre-concentration conditions that yielded colloidal microchannel formation in Figure 2c. Importantly, all the data points shown in Figure 2c and Figure 3 were based on experimental observations. There are 180 different combinations of temperature and concentrations in Figure 2c and Figure 3 (e.g., temperature 20℃, 25℃, 30℃… 90℃ and concentration 10%, 20%... 100%), obtained from 540 experiments (i.e., 3 repeated experiments for each combination). As the temperature increased, the difference in the thickness from outer to inner part of the film was smaller. Therefore, colloidal microchannel still formed at relative low concentration (i.e., concentration 30%). In contrast, at lower temperature (e.g., 20℃), the boundary concentration is 50%. For tempearture above 50℃, the boundary concentration stayed at 30%, same as 50℃, suggesting that it is impossible to generate a colloidal film with uniform film thickness by simply tuning the temperature. This might be due to the different evporation rate of droplet with different sizes.

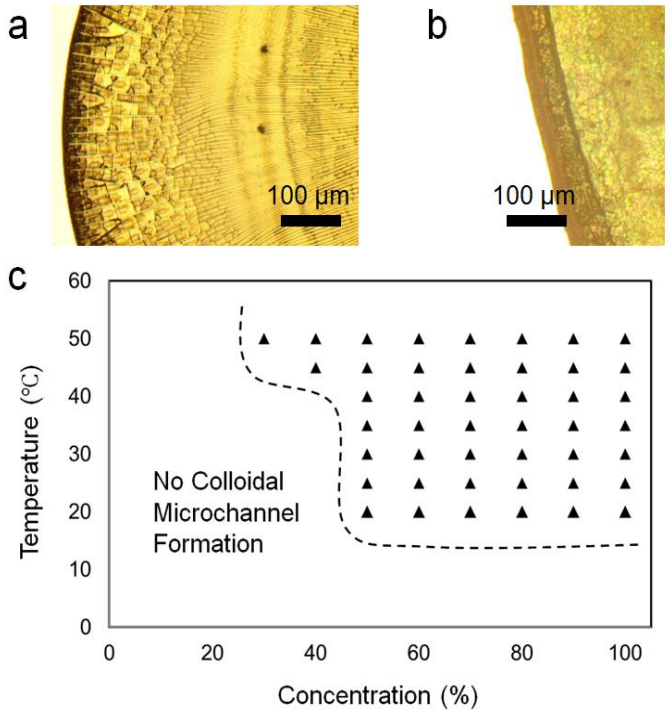

FIGURE 2: Optical microscope images of (a) colloidal microchannel formed through the drying of colloidal film of 50 nm PS latex nanoparticles and (b) giant ring-like deposition of PS latex nanoparticles with no colloidal microchannel formation. (c) temperature-concentration phase diagram of colloidal microchannel formation of 50 nm PS latex nanoparticles. Notably, concentration 100% means 2.5 wt% of PS latex nanoparticle aqueous solution and 40% means 0.4*2.5=1wt% PS latex nanoparticle aqueous solution.

Surprisingly, we observed a distinct temperature-concentration phase diagram (Figure 3) when the size of PS latex nanoparticle increased to 100 nm, compared to the phase diagram of 50 nm. First, at temperature around 20℃, we could not notice colloidal microchannel formation for 100 nm PS latex nanoparticle, which is noticeable for 50 nm. Second, even at relatively low concentration (e.g., 10%, which is 0.25 wt%), there was still colloidal microchannel formation. However, intriguingly, when concentration is in the range of 60%~100% for temperature lower than 35℃. All above mentioned differences yield a colloidal microchannel formation area located in the upper left in the phase diagram of 50 nm PS latex nanoparticle while in the upper right of phase diagram of 100 nm

We attribute the major differences between the two-phase diagrams (as shown in Figure 2c and Figure 3) to the dual role of "coffee-ring" effect. It is noteworthy that the outward flux generated by the "coffee-ring" effect should be the same for PS latex nanoparticle solution for both sizes (i.e., 50 nm and 100 nm), because we used the solution volume for both cases (i.e., 15 μL) and the droplet size was not affected by the particle size. The first role "coffee-ring" effect plays is to transport PS latex nanoparticles from the bulk solution to the three-phase contact

line. As the 100 nm PS latex nanoparticle is four times heavier than the 50 nm, it is harder for the evaporative flux to carry larger particles to the contact line. It is known that the "coffee-ring" effect will be enhanced as temperature increases, due to the increased evaporation rate.[46] Therefore, it is shown that there are sufficient bigger PS latex nanoparticles (100 nm) transported to the edge to form colloidal microchannels at elevated temperature (e.g., above 40℃). However, for higher concentration with lower temperature (concentration above 50% and temperature below 35℃), the "coffee-ring" effect induced outward flux is not strong enough to carry large numbers of particles for colloidal film formation, resulting in no or much less colloidal microchannel formation.

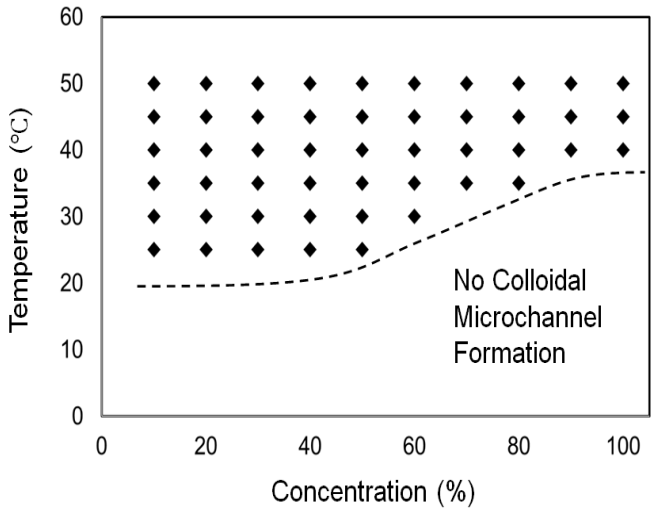

FIGURE 3: Temperature-concentration phase diagram of colloidal microchannel formation of 100 nm PS latex nanoparticles.

In contrast, the transportation by outward flux is not an issue for smaller PS particles (50 nm). However, the aggregation of smaller PS particles due to "coffee-ring" effect becomes an issue, which leads to the discovery of the second role the "coffee-ring" effect plays during colloidal microchannel formation: to accumulate particles at the contact line. Due to the "coffee-ring" effect induced accumulation, there is no continuous colloidal film formation at lower concentration for smaller PS latex nanoparticles. As a result, a giant ring-like deposition formed at the edge as shown in Figure 1b, leading to no microchannel formation. Clearly, the smaller the particles are, the stronger accumulation there will be. Even though by varying the particle shape, such accumulation induced by "coffee-ring" effect could be reduced, it will also significantly change the colloidal microchannel formation process due to the anisotropic internal stress disctribution.[47]

4. CONCLUSION

In summary, by understanding the dual roles of the "coffee-ring" effect plays during colloidal microchannel formation, we found that the large particles (100 nm) help to smooth out the overall deposited film thickness, leading to more uniform colloidal microchannel formation, but requires stronger "coffee-ring" effect. In contrast, the small particles could be easily transported to the contact line by weak "coffee-ring" effect at lower temperatures. However, the small particles form large aggregations at the edge which results in large pinning force, and, consequently, causes the failure of colloidal microchannel formation. As a result, the dual roles of the "coffee-ring" effect render two distinct temperature-concentration phase diagrams of colloidal microchannel formation for PS latex nanoparticles with two different sizes. The complex relationship between "coffee-ring" effect and particle size has been found for the first time in this work. The particle size not only determine the internal stress which drives colloidal cracking as demonstrated in previous work, but also greatly influence the particle transportation process, which changes both the uniformity of the film thickness and the pinning force of the droplet. The presented study in this work offers key insights for tuning particle size for colloidal microchannel formation, benefiting advanced manufacturing based on self-assembly of colloidal nanoparticles.

ACKNOWLEDGEMENTS

We thank the support of Undergraduate Research & Creative Activities (URCA) Funding Award at Kennesaw State University.

REFERENCES

[1] Pang, X.; He, Y.; Jung, J.; Lin, Z., *Science* **2016,** *353* (6305), 1268-1272.
[2] Pang, X.; Zhao, L.; Han, W.; Xin, X.; Lin, Z., *Nat Nano* **2013,** *8* (6), 426-431.
[3] Whitesides, G. M.; Grzybowski, B., *Science* **2002,** *295* (5564), 2418-2421.
[4] Bishop, K. J. M.; Wilmer, C. E.; Soh, S.; Grzybowski, B. A., *Small* **2009,** *5* (14), 1600-1630.
[5] Liao, L.; Lin, Y.-C.; Bao, M.; Cheng, R.; Bai, J.; Liu, Y.; Qu, Y.; Wang, K. L.; Huang, Y.; Duan, X., *Nature* **2010,** *467* (7313), 305-308.
[6] Nie, Z.; Petukhova, A.; Kumacheva, E., *Nat Nano* **2010,** *5* (1), 15-25.
[7] Piner, R. D.; Zhu, J.; Xu, F.; Hong, S.; Mirkin, C. A., *Science* **1999,** *283* (5402), 661-663.
[8] Guan, J.; Lee, L. J., *P. Natl. Acad. Sci. Usa.* **2005,** *102* (51), 18321-18325.
[9] Li, B.; Han, W.; Byun, M.; Zhu, L.; Zou, Q.; Lin, Z., *ACS Nano* **2013,** *7* (5), 4326-4333.
[10] Han, W.; Byun, M.; Li, B.; Pang, X.; Lin, Z., *Angew. Chem., Int. Ed.* **2012,** *51* (50), 12588-12592.
[11] Hawker, C. J.; Russell, T. P., *MRS Bull.* **2005,** *30* (12), 952-966.
[12] Jang, Y.; Jo, J.; Kim, D.-S., *J. Polym. Sci. Pol. Phys* **2011,** *49* (22), 1590-1596.
[13] Alexander, F. R., *Rep. Prog. Phys.* **2013,** *76* (4), 046603.
[14] Allain, C.; Limat, L., *Phys. Rev. Lett.* **1995,** *74* (15), 2981-2984.
[15] Jagla, E. A., *Phys. Rev. E* **2002,** *65* (4), 046147.

[16] Lidon, P.; Salmon, J.-B., *Soft Matter* **2014,** *10* (23), 4151-4161.
[17] Tirumkudulu, M. S.; Russel, W. B., *Langmuir.* **2005,** *21* (11), 4938-4948.
[18] Han, W.; Li, B.; Lin, Z., *ACS Nano* **2013,** *7* (7), 6079-6085.
[19] Deegan, R. D.; Bakajin, O.; Dupont, T. F.; Huber, G.; Nagel, S. R.; Witten, T. A., *Nature* **1997,** *389* (6653), 827-829.
[20] Langmuir, I., *Phys. Rev.* **1918,** *12* (5), 368-370.
[21] Cazabat, A.-M.; Guena, G., *Soft Matter* **2010,** *6* (12), 2591-2612.
[22] Hu, H.; Larson, R. G., *J. Phys. Chem. B* **2002,** *106* (6), 1334-1344.
[23] Deegan, R. D., *Phys. Rev. E* **2000,** *61* (1), 475.
[24] Deegan, R. D.; Bakajin, O.; Dupont, T. F.; Huber, G.; Nagel, S. R.; Witten, T. A., *Phys. Rev. E* **2000,** *62* (1), 756-765.
[25] Fischer, B. J., *Langmuir.* **2001,** *18* (1), 60-67.
[26] Bhardwaj, R.; Fang, X.; Somasundaran, P.; Attinger, D., *Langmuir.* **2010,** *26* (11), 7833-7842.
[27] Anyfantakis, M.; Baigl, D., *Angew. Chem. Int. Ed.* **2014,** *126* (51), 14301-14305.
[28] Hamamoto, Y.; Christy, J.; Sefiane, K., *Phys. Rev. E* **2011,** *83* (5), 051602.
[29] Harris, D. J.; Hu, H.; Conrad, J. C.; Lewis, J. A., *Phys. Rev. Lett.* **2007,** *98* (14), -.
[30] Gleiche, M.; Chi, L. F.; Fuchs, H., *Nature* **2000,** *403* (6766), 173-175.
[31] Chi, L. F.; Rakers, S.; Hartig, M.; Gleiche, M.; Fuchs, H.; Schmid, G., *Colloid Surface. A* **2000,** *171* (1-3), 241-248.
[32] Prevo, B. G.; Velev, O. D., *Langmuir.* **2004,** *20* (6), 2099-2107.
[33] Yabu, H.; Shimomura, M., *Adv. Funct. Mater.* **2005,** *15* (4), 575-581.
[34] Xu, J.; Xia, J. F.; Hong, S. W.; Lin, Z. Q.; Qiu, F.; Yang, Y. L., *Phys. Rev. Lett.* **2006,** *96* (6), -.
[35] Xu, J.; Xia, J.; Lin, Z., *Angew. Chem. Int. Ed.* **2007,** *119* (11), 1892-1895.
[36] Hong, S. W.; Byun, M.; Lin, Z. Q., *Angew. Chem. Int. Ed.* **2009,** *48* (3), 512-516.
[37] Hong, S. W.; Giri, S.; Lin, V. S. Y.; Lin, Z. Q., *Chem. Mater.* **2006,** *18* (22), 5164-5166.
[38] Hong, S. W.; Jeong, W.; Ko, H.; Kessler, M. R.; Tsukruk, V. V.; Lin, Z. Q., *Adv. Funct. Mater.* **2008,** *18* (14), 2114-2122.
[39] Hong, S. W.; Wang, J.; Lin, Z. Q., *Angew. Chem. Int. Ed.* **2009,** *48* (44), 8356-8360.
[40] Hong, S. W.; Xia, J. F.; Byun, M.; Zou, Q. Z.; Lin, Z. Q., *Macromolecules* **2007,** *40* (8), 2831-2836.
[41] Hong, S. W.; Xia, J.; Lin, Z., *Adv. Mater.* **2007,** *19* (10), 1413-1417.
[42] Hong, S. W.; Xu, J.; Lin, Z. Q., *Nano Lett.* **2006,** *6* (12), 2949-2954.
[43] Hong, S. W.; Xu, J.; Xia, J. F.; Lin, Z. Q.; Qiu, F.; Yang, Y. L., *Chem. Mater.* **2005,** *17* (25), 6223-6226.
[44] Routh, A. F.; Russel, W. B., *Langmuir.* **1999,** *15* (22), 7762-7773.
[45] Li, B.; Jiang, B.; Han, W.; He, M.; Li, X.; Wang, W.; Hong, S. W.; Byun, M.; Lin, S.; Lin, Z., *Angewandte Chemie International Edition* **2017,** *56* (16), 4554-4559.
[46] Li, B.; Iocozzia, J.; Lin, Z., Directing Convection to Pattern Thin Polymer Films: Coffee Rings. In *Polymer Surfaces in Motion: Unconventional Patterning Methods*, Rodríguez-Hernández, J.; Drummond, C., Eds. Springer International Publishing: Cham, 2015; pp 43-71.
[47] Yunker, P. J.; Still, T.; Lohr, M. A.; Yodh, A. G., *Nature* **2011,** *476* (7360), 308-311.